Soil Biology and Biochemistry 143 (2020) 107742

Contents lists available at ScienceDirect

Soil Biology and Biochemistry

journal homepage: http://www.elsevier.com/locate/soilbio

Microbial extracellular polysaccharide production and aggregate stability controlled by switchgrass (*Panicum virgatum*) root biomass and soil water potential

Yonatan Sher [a,1], Nameer R. Baker [b,1,*], Don Herman [b,c], Christina Fossum [b], Lauren Hale [d], Xingxu Zhang [e], Erin Nuccio [f], Malay Saha [g], Jizhong Zhou [c,h], Jennifer Pett-Ridge [f], Mary Firestone [b,c]

[a] Migal Galilee Research Institute, Kiryat Shmona, Israel
[b] University of California, Berkeley, CA, USA
[c] Lawrence Berkeley National Laboratory, Berkeley, CA, USA
[d] USDA-Agricultural Research Service, Parlier, CA, USA
[e] Lanzhou University, Lanzhou, China
[f] Lawrence Livermore National Laboratory, Livermore, CA, USA
[g] Noble Research Institute, Ardmore, OK, USA
[h] University of Oklahoma, Norman, OK, USA

ARTICLE INFO

Keywords:
EPSac
Marginal soil
Stable soil aggregate
Switchgrass
Root biomass
^{13}C labeling

ABSTRACT

Deep-rooting perennial grasses are promising feedstocks for biofuel production, especially in marginal soils lacking organic material, nutrients, and/or that experience significant water stress. Perennial grass roots influence surrounding soil conditions and microbial activities, and produce extracellular polymeric substances (EPS) composed primarily of extracellular polysaccharides (EPSac). These polymers can alleviate microbial moisture and nutrient stress, and enhance soil characteristics through improved water retention and aggregate stability—which may in turn enhance carbon persistence. In this study we used a $^{13}CO_2$ greenhouse tracer experiment to examine the effect of switchgrass cultivation on EPSac production and origin in a marginal soil with five fertilization/water treatments (control, +N, +NP, +P, low water), and compared these results with measurements of field soils collected after long-term switchgrass cultivation. Soils with added nitrogen and phosphorus (+NP) had the highest root biomass, EPSac and percentage of water-stable soil aggregates. Multiple linear regression analyses revealed that root biomass and soil water potential were important determinants of soil EPSac production, potentially by controlling carbon supply and diurnal changes in moisture stress. Path analysis showed that soil aggregation was positively correlated with bulk soil EPSac content and also regulated by soil water potential. High mannose content indicated the majority of EPSac was of microbial origin and $^{13}CO_2$ labeling indicated that 0.18% of newly fixed plant carbon was incorporated into EPSac. Analysis of field soils suggests that EPSac is significantly enhanced after long-term switchgrass cultivation. Taken as a whole, our greenhouse and field results demonstrate that switchgrass cultivation can promote microbial production of EPSac, providing a mechanism to enhance aggregation in marginal soils.

1. Introduction

Soil microorganisms are known to produce extracellular polymeric substances (EPS) to adhere to surfaces and protect themselves from external stresses (Cheshire, 1977; Sandhya and Ali, 2015; Wolfaardt et al., 1999); such substances may take on added importance in the relatively low-nutrient and variable-moisture environments present in marginal soils. These polymeric substances include a variety of biological polymers, such as DNA and proteins, but the principal components are typically polysaccharides (Cheshire, 1977; More et al., 2014; Oades,

* Corresponding author.
E-mail addresses: nameer@berkeley.edu (N.R. Baker), mkfstone@berkeley.edu (M. Firestone).
[1] equal contribution.

https://doi.org/10.1016/j.soilbio.2020.107742
Received 6 August 2019; Received in revised form 28 January 2020; Accepted 3 February 2020
Available online 7 February 2020

1984). Physical and chemical characteristics of extracellular polysaccharides (EPSac) help microbial cells alleviate moisture and nutrient stress, and could enhance the formation of soil aggregates that are lacking in marginal soils. Due to their high water-absorption and retention capacity (Adessi et al., 2018; Sandhya and Ali, 2015), EPSac reduce the stress of low soil water potential on microbial cells. Enhanced soil water holding capacity can increase nutrient diffusion to and from microbial cells encased in EPSac (Chenu and Roberson, 1996). The sticky, gelatinous properties of EPSac also bind microbial cells to soil mineral surfaces (Wolfaardt et al., 1999) and enhance soil-aggregation by binding soil particles together (Costa et al., 2018; Martin, 1946; Oades, 1984) into aggregates (Six et al., 2000; Six and Paustian, 2014; Tisdall and Oades, 1982). EPSac thus enhance the formation of water-stable aggregates (Sandhya and Ali, 2015) and increase mean soil aggregate size (Amellal et al., 1999), which can enhance the persistence of organic C by occluding it within aggregates (Jastrow et al., 2007). EPSac may also directly increase C persistence in soil by binding to soil mineral surfaces occluded in pores at the submicron scale that are unavailable for microbial consumption (Chenu and Cosentino, 2011; Liang et al., 2017; von Lützow et al., 2006).

Microbial EPSac production tends to increase during dry periods, as microbes produce more EPSac to enhance water retention of the surrounding soil matrix (Roberson and Firestone, 1992). As such, we would expect to see more EPSac produced in drier or variable-moisture soil conditions. EPSac production is also sensitive to changes in temperature, pH, and salinity (Ali et al., 2009; Jiao et al., 2010; Upadhyay et al., 2011). Nutrient availability is strongly correlated with microbial EPSac production, since the availability of different carbon (C) sources directly influences the precursor molecules available to be anabolized into EPSac (Celik et al., 2008). Lack of nitrogen (N) or phosphorus (P), inferred from a high C:N ratio, has also been shown to positively affect EPSac production by soil microbial isolates (Roberson, 1991; Staudt et al., 2012). Thus, microbial production of EPSac may be enhanced in marginal soils that commonly possess low N content, but could also be limited by C availability given a lack of available organic material.

Cultivation of perennial grasses as cellulosic feedstocks on marginal lands is expected to have a central role in climate change mitigation (Abraha et al., 2019; Robertson et al., 2017). Perennial plants have significant carbon balance benefits relative to other potential biofuel feedstocks such as corn (Gelfand et al., 2011; Tilman et al., 2006). Perennial grasses such as switchgrass (*Panicum virgatum*, hereafter SG) possess extensive rooting systems that persist over multiple growing seasons in the soil (Chimento et al., 2016; Ontl et al., 2015). These roots provide C to rhizosphere microbial communities in the form of root exudates, mucilage (Mao et al., 2014) and decomposing root litter (Jackson et al., 1997), and may cause the liberation of mineral-associated C by exuded organic acids (Keiluweit et al., 2015). In a marginal soil context, where organic matter and nutrients are often limiting, root C inputs may alleviate C-limitation for microbial communities, and have been shown to facilitate macroaggregation when added to subsoil via artificial roots (Baumert et al., 2018).

Perennial rooting systems can insert plant C deeper into the soil profile than annual plants, potentially increasing a soil's capacity to sequester C at depth (Anderson-Teixeira et al., 2009; Tilman et al., 2006). Notably, perennial grasses significantly enhance soil aggregation under long-term cultivation (Jastrow et al., 1998; Ontl et al., 2015), and aggregated soils store C more effectively than those in which structure is lacking (Liao et al., 2006; McGowan et al., 2019). In addition, studies show that switchgrass (SG) biomass in the field is often not enhanced by nutrient amendments in marginal soils (Brejda, 2000; Parrish and Fike, 2005, Thomason et al., 2005), which makes its cultivation on such soils more cost-effective. This raises the question of whether there are mutualistic relationships between SG roots and their associated soil microbial community that alleviate the nutrient deficits in these soils (Rodrigues et al., 2017). In particular, SG may directly facilitate microbial production of EPSac by providing microbes with labile C precursors (Mao et al., 2014) and indirectly enhance EPSac production by altering soil water potential through root uptake and potentially through hydraulic lift (Caldwell et al., 1998).

In this study, we grew SG in a 'marginal' sandy loam soil (lacking in nutrients and C) and manipulated nutrient and moisture availability in a greenhouse experiment to test the hypothesis that soil microbial communities would produce more EPSac when exposed to greater abiotic stress. We hypothesized that treatments that enhanced EPSac production would also enhance the formation of water-stable aggregates, given the adhesive properties of EPSac. To assess the broader relevance of our greenhouse results, we also tested the hypothesis that field cultivation of SG enhances soil EPSac content (relative to annual cereal crops). Our objective was to determine if SG cultivation can alter microbial activity and enhance beneficial soil characteristics, such as aggregate stability, that are lacking in marginal soils.

2. Methods

2.1. Soil collection and preparation

Soils were collected from a pasture soil in Caddo County, OK, near the town of Anadarko (35.072417/-98.303667), where switchgrass is endemic. The soil, described by the USDA soil series as Pond Creek fine sandy loam with 1–3 percent slopes, is classified as a superactive, thermic Pachic Argiustoll (Moffatt, 1973) and an arenic Plaggic Anthrosol according to the World Reference Base soil classification system (IUSS, 2015). We consider it to be a marginal soil because of its low C content (<0.4% total C), low nutrient content (<0.04% total N, < 6 ppm total P), and high (>70%) sand content in all three observed horizons down to 1 m in depth (Table S1). In November of 2016, a Caterpillar backhoe with a 60" digging shovel was used to excavate 1-m deep soil pits. In this range, the soil profile was characterized as having three distinct horizons– an A horizon with noticeably more organic material in the top 25 cm, a B horizon with greater sand content from 25 to 70 cm, and a deeper, noticeably denser C horizon from 70 cm and below. Bulk density cores were also taken from each horizon (Table S1).

After removing living plant material from the surface (0–3 cm), approximately ~4 m^3 of soil was collected from each horizon using the same backhoe and transported to our greenhouse facility at the University of California, Berkeley (UCB). Soils were stored indoors and in December 2016, soil from each horizon was homogenized in a 0.255 m^3 cement mixer and then stored in sandbags for 2 months at ambient conditions (25 °C during the day and 18 °C overnight). Sub-samples were taken from each homogenized horizon for initial soil chemistry assays (Table S1). Bulk density cores were weighed fresh and dried at 70 °C until no change in soil weight was observed to assess field bulk density of each horizon.

We also conducted soil coring campaigns to compare bulk soil EPSac content with depth in long-term perennial SG fields (10–20 years) and in adjacent annual crop fields. Soil coring campaigns were conducted at the Noble Research Institute (NRI) Red River field site (10-year SG cultivation) and at a field site near Stillwater, OK (20-year SG cultivation). Soil cores were excavated using a Giddings probe (Giddings Machine Company, Windsor, CO). Soil core tubes, ~10 cm diameter and ~1.2 m length (with a 9 cm diameter Zero Contamination system liner), were used to progressively collect soil cores from up to ~3 m depth, for three replicate 1.2 m cores. Each 1.2 m core was cut into three sections of ~30 cm, and soil from the bottom 20 cm of each section was stored at 4 °C for one week before EPSac were extracted and quantified.

2.2. Mesocosm preparation, experimental design and SG cultivation

For our greenhouse mesocosm study, soil profiles were re-created based on field observations, with homogenized soil horizons packed into 30 clear, impact-resistant polycarbonate cylinders (hereafter referred to as "mesocosms"), 122 cm in length and 19.7 cm in diameter.

In each mesocosm, we added the A, B, and C soil to allow each horizon 33 cm of vertical depth, packed at field bulk density. At the base, each cylinder was sealed with a custom-fitted polycarbonate cap and 500 g of coarse-grained sand to provide drainage. During packing, an anion exchange resin membrane (Membranes International, Ringwood, NJ) was added to the center of each horizon. These were designed to provide a cumulative measure of available PO_4^{3-} in that horizon by absorbing PO_4^{3-} at a rate proportional to its concentration in the soil solution and retaining it until assayed.

To establish five experimental treatments, before adding the A horizon soil to the mesocosm, it was mixed in a cement mixer for 2 min with: no additions (control and low water treatments), added N (+N), added P (+P), or combined N and P (+NP) amendments (Fig. S1A). N was added in the form of 0.13 g kg^{-1} dry soil of ESN Smart Nitrogen slow-release coated urea (44-0-0, Agrium) in accordance with the recommendations provided by Oklahoma State University's Division of Agricultural Sciences and Natural Resources for high biomass SG cultivation, equivalent to 84 kg ha^{-1} (Arnall et al., 2018). P (0.48 g kg^{-1}) was added in the form of slow-release rock phosphate (0-3-0, Espoma) to bring the total concentration of plant extractable P up to 20 ppm, which resulted in an amendment consistent with manufacturer recommendations as well as Oklahoma State University's recommendations for SG cultivation in soils with ~5 ppm of total phosphorus, equivalent to 22 kg ha^{-1} (Arnall et al., 2018).

Completed mesocosms (six replicates x five treatments = 30 mesocosms) were wrapped in black high-density polyethylene sheeting and then white polypropylene sacking (to prevent soil temperatures from being elevated by solar radiation) and stored for an additional five weeks before planting with SG. Soil moisture probes (EC-20; METER Group, Pullman, WA) were installed in the A horizon of the control and low water treatments mesocosms to maintain target moisture conditions. To re-hydrate the soil profile and allow it to equilibrate before planting, 2 L of deionized H_2O was added to each mesocosm every week, until the A horizon reached 80% of field-holding capacity the day after watering.

A SG genotype, NFSG 18-01, from the Nested Association Mapping population (NAM) with established high biomass productivity in both Oklahoma and Tennessee was selected for this experiment. SG is highly heterogeneous, and every plant is genetically distinct. To avoid any genetic variation among treatments and replicates, we used a single clone for this experiment. The plant was grown in the Noble Research Institute (NRI) greenhouse at 32 °C (daytime)/21 °C (nighttime) and 16 h photoperiod for maximum growth. A total of 120 clonal ramets were prepared from one plant and shipped to UCB. Uniform ramets of NFSG 18-01 were planted into each of the 30 mesocosms in early May 2017, with extras planted into conical planters to replace failed plantings. Mesocosms were arranged in 6 wheeled stainless-steel caddies in sets of five (one of each treatment, in random order), making each caddy equivalent to a "plot." Thereafter, mesocosms were watered with 100 ml of deionized H_2O daily—roughly equivalent to the rainfall experienced in NRI field plots in southern Oklahoma in the higher precipitation months of May and June. After two weeks, no planted SG appeared to be failing, so after another two weeks (four weeks total) plants were considered to be established within the mesocosms and watering for the low water treatment was reduced to 50 ml of H_2O daily. After eight weeks, the temperature in the green house was increased to 32 °C (daytime)/21 °C (nighttime) to simulate growing season conditions in Oklahoma.

2.3. $^{13}CO_2$ pulse-chase labeling

After plants had grown for 18 weeks, we performed a 12-day $^{13}CO_2$ pulse-chase labeling to track plant photosynthate C into EPSac and bulk soil (Fig. S1B). Half (15) of the mesocosms from each treatment were labeled with $^{12}CO_2$ (Praxair, Danbury, CT) as controls for future stable-isotope probing (SIP) and the other half were labeled with 99 atom-percent $^{13}CO_2$ (Cambridge Isotope Laboratories, Tewksbury, MA), providing three replicates of each treatment under each labeling regime. Labeling was carried out using a custom apparatus consisting of a Picarro G2131-I Analyzer (Santa Clara, CA) and Infrared Gas Analyzer, (IRGA, Campbell Scientific, Logan, UT) combined with a CR1000 Datalogger (Campbell Scientific, Logan, UT) to enable real-time assessment of [$^{12}CO_2$] and [$^{13}CO_2$] in up to 32 chambers (16 of each type of CO_2).

2.4. Harvest of plant biomass and processing of soils for analysis

After the September 2017 pulse-labeling, $^{13}CO_2$ enriched mesocosms were destructively harvested by clipping SG shoots at the soil surface and partitioning soil horizons for sample collection. For each soil horizon, roots and closely-associated soil (<2 mm from root) were collected by hand, washed in deionized water, and dried at 70 °C until no change in root weight was observed. All measures of gravimetric water content, pH, and soil chemistry and all extractions of EPSac presented in this study were performed on fresh bulk soil (>2 mm from roots) that was stored at 4 °C after collection. Bulk soil was also aliquoted for assessment of water-stable aggregates and air-dried in open bags. Gravimetric soil water content was measured for each horizon of each replicate by drying fresh bulk soil at 70 °C until no change in soil weight was observed. Soil water content was converted to soil water potential with water retention curves generated from air-dried samples from each horizon using a pressure plate apparatus (WP4C, METER Environment, Pullman, WA) and a van Genuchten model to apply a non-linear fit to the data (Seki, 2007). Volumetric soil water content measured by EC-20 probes in the A horizon of the control and low water treatments was also converted to soil water potential using these water retention curves.

To assess dissolved organic carbon (DOC) and total dissolved nitrogen (DN), 5 g fresh bulk soil was extracted with 20 ml 0.5 M K_2SO_4. DOC and DN in the 0.5 M K_2SO_4 extract were measured using a Shimadzu TOC-L analyzer coupled with a TNM detector (Kyoto, Japan). Soil pH values were determined in slurries made by mixing 5 g of soil with 5 ml of 0.01 M $CaCl_2$. 1 g dried soil was sent to Oregon State University's Central Analytical Laboratory (Corvallis, OR) for total C quantification by combustion at 1150 °C on an Elemental Macro Cube. PO_4 accumulation on ion exchange resin membranes was assessed by extracting anions with 0.5 M HCl and assessing the ppm of P in the extract with a microplate reader using methods described by D'Angelo et al. (2001).

2.5. EPSac extraction and analysis

We modified a cation exchange resin (CER) extraction method (Redmile-Gordon et al., 2014; Wang et al., 2019) to examine EPSac content in bulk soil samples. The CER reduces binding between multivalent cations and polymeric substances (Sheng et al., 2010), releasing EPSac into the extraction buffer solution. This approach minimizes microbial cell lysis that can potentially bias the results (Redmile-Gordon et al., 2014; Wang et al., 2019), and maximizes extracted EPSac yield (Frølund et al., 1996; Sheng et al., 2010). Combining this CER extraction with an ethanol precipitation step isolates high molecular weight carbohydrates (Chang et al., 2007), thus targeting soil carbohydrates that are both extracellular and polymeric - i.e., EPSac.

In our modified extraction method, the extraction buffer was changed to phosphate buffer saline (PBS; Gibco, Grand Island, NY). 5 g of soil (stored at 4 °C until extraction) together with 10 ml PBS were added to a 50 ml tube containing 1 g CER (Dowex® Marathon® C, 20–50 mesh, Na^+ form, Sigma-Aldrich, St. Louis, MO). This slurry was shaken for 30 min at 4 °C and subsequently centrifuged at 3000 rpm for 10 min at 4 °C. The supernatant was passed through a 0.2 μm nylon filter, and polysaccharides were precipitated from the filtrate with three volumes of 100% ethanol and concentrated 10x (Chang et al., 2007).

To extract EPSac for ^{13}C analysis, the extraction procedure was upscaled 18x to obtain enough C in the extract to allow for isotope

enrichment (IRMS) analysis. Extracts were precipitated twice in ethanol, to reduce the sample volume to 1 ml. Reduced volume extracts were transferred to small tin cups (Costech, Valencia, CA) and evaporated to complete dryness at 70 °C. These tin cups were then prepared for IRMS analysis, as described in section 2.8.

Total EPSac was quantified by measuring carbohydrates with a sulfuric acid/phenol method (DuBois et al., 1956), modified for microplates. A colorimetric reaction mix composed of 50 μl of each EPSac sample (or standard), 150 μl sulfuric acid (95–98%, A300-212, Fisher Chemical), and 30 μl 5% phenol (Spectrum chemicals) was added to a 1 ml well in a 96 well polypropylene deep-well plate (Thermo Scientific Nunc, Waltham, MA, USA). Plates were tightly covered with a polypropylene lid and placed on a micro-plate block heater for 45 min at 100 °C, then allowed to cool for 15 min 100 ml of the mix was transferred from each well of the polypropylene plate to a clear, flat bottom, polystyrene 96 well microplate (Greiner Bio-One) and placed in Spectramax plus 384 plate reader (Molecular Devices) to measure absorbance at 490 nm. Carbohydrate content was measured against a calibration curve of glucose in the range of 0.5–250 μg ml^{-1} (Chang et al., 2007).

To assess the monosaccharide composition of EPSac, 20 μg ml^{-1} solutions of each EPSac extract were generated. These solutions were hydrolyzed by adding an equal volume of 4 M trifluoroacetic acid (TFA; Sigma-Aldrich) to attain a 2 M final concentration, before being incubated for 90 min at 121 °C. Hydrolysates were washed twice with isopropanol by evaporating isopropanol with a TECHNE sample concentrator (Cole-Parmer Ltd., UK), and were then eluted with 0.5 ml ultrapure water. Re-suspended samples were centrifuged for 10 min at 13,000×*g* at 4 °C, to remove solids, and 80% of the supernatant was collected for analysis. Monosaccharide composition was measured with a Dionex ICS-3000 ion chromatography system with CarboPac™ PA20 column (Thermo Fisher Scientific). Samples were analyzed in two runs with two KOH eluent concentrations, 2 mM and 18 mM, as the arabinose and rhamnose peaks overlap at 2 mM and the xylose and mannose peaks overlap at 18 mM (Yeats et al., 2016). We used this data to calculate the ratio of hexose to pentose sugars in extracted EPSac to verify its microbial origin (Gunina and Kuzyakov, 2015; Oades, 1984). It is recommended to assess EPSac monosaccharide composition in the context of the plant being studied (Gunina and Kuzyakov, 2015), so we also sampled SG roots from NRI's Red River field site (Burneyville, OK, 33.882235/-97.275919) in early May 2017 to calculate the hexose to pentose ratio in polysaccharides from SG root mucilage. EPSac extraction and assessment of monosaccharide composition was performed both on roots and bulk soil samples from this site. EPSac extraction from bulk soil was performed as described above. EPSac extraction from roots was performed by washing them with PBS, filtering the supernatant through a 0.2 μm filter, and precipitating the resulting EPSac with 100% ethanol.

2.6. Soil aggregate stability

Soil aggregate stability was measured with a single wet sieving method (Kemper and Rosenau, 1986) on 1–2 mm soil aggregates. Air-dried soil was passed through a 2 mm sieve and collected on a 1 mm sieve to generate the 1–2 mm aggregates. 5 g of aggregates were placed on a 0.25 mm sieve and repeatedly dunked in a water cup for 5 min, using a mechanical dunking apparatus (Singer et al., 1992). The mass of the unstable aggregates (those that dispersed) and the stable aggregates (those that stayed on the sieve) was measured after drying at 70 °C. The following ratio was used as the measure for soil aggregate stability:

$$\frac{stable\ aggregates}{(stable\ aggregates) + (unstable\ aggregates)}$$

Before assessing soil aggregate water-stability, all soil samples from all treatments were air-dried and had consistent low soil water content to avoid confounding the assay.

2.7. Phospholipid fatty acid analysis (PLFA)

Microbial biomass in each soil sample was determined by Phospholipid Fatty Acid (PLFA) analysis, with a high throughput 96 well plate method to extract and trans-esterify PLFAs, as described by Buyer and Sasser (2012). PLFAs were extracted from 2 g dry soil samples from the greenhouse experiment; in the B and C horizons, extracts of two 2 g dry soil samples were combined. After transesterification steps, Fatty Acid Methyl Esters (FAMEs) were then analyzed by gas chromatography (Agilent Technologies, Wilmington, DE, USA) and identified using the MIDI Sherlock Microbial Identification System (MIDI Inc, Newark, DE, USA). An internal standard,19:0 phosphatidylcholine (Avanti Polar Lipids, Alabaster, AL, USA), and chromatogram peaks of a PLFAD1 calibration mix and peak library (MIDI Inc, Newark, DE, USA) were used to calculate the concentration of analyzed PLFAs and total microbial biomass using MIDI's recommended allocation by category (Supplemental file MICSOIL3.txt). Community structure cannot be inferred reliably using this method when total microbial biomass is low; as such, we did not assess microbial community structure in this study.

2.8. ^{13}C analysis

^{13}C in both bulk soil samples and EPSac extracts from the surface horizon were analyzed with an IsoPrime 100 continuous flow isotope ratio mass spectrometer (IRMS) interfaced with a trace gas analyzer (Isoprime Ltd, Cheadle Hulme, UK). ^{13}C enrichments were calculated by subtracting ^{13}C atom% natural abundance (found in control ^{12}C treatments) from the total ^{13}C atom% found in ^{13}C treatments. ^{13}C atom% was multiplied by either total C per g soil for each soil sample, to calculating the amount of labeled soil C, or by EPSac per g soil, to calculate the amount of labeled EPSac.

2.9. Statistical analysis

Statistical analysis and data visualization were conducted with R version 3.6.0 (R Core Team, 2018). Significant differences in soil properties and SG root biomass between treatments and soil horizons for the greenhouse study and differences in EPSac content between SG and annual crop fields with depth were determined by ANOVA. Every two adjacent depths from the field samplings were combined during analysis to increase statistical power. Significant differences in microbial biomass between treatments and soil horizons were assessed for the A and B horizon only, given the prevalence of N/A results for PLFA microbial biomass in the C horizon. For further multiple comparisons between treatments and soil horizons, pairwise t-tests were conducted without pooled standard deviations (Welch's *t*-test), as the assumption of equal variance between samples for Tukey's test were not met for some of the analyses. To correct for multiple testing, the Benjamini-Hochberg correction was used (Benjamini and Hochberg, 1995). Box-whisker graphs were built with the ggplot2 package (Wickham, 2016) in R. Significant differences in EPSac monosaccharide composition as a result of treatment were determined by MANOVA.

To determine which measured properties best explain EPSac and soil aggregate stability variability between treatments and horizons, we employed multiple linear regression analysis. Multicollinearity between examined factors was detected by calculating the variance inflation factor (VIF) between them (Fox and Weisberg, 2011), and removing highly correlated factors with VIF value above 3 (Zuur et al., 2010) in a stepwise manner. After removing highly correlated factors, factors with low explanatory significance to the multiple linear regression models were removed after Akaike Information Criterion (AIC) estimation of the relative quality of the models (Venables and Ripley, 2002). Correlation between factors was visualized with correlation matrix charts (Peterson et al., 2018) (Fig. S2, S3).

We used path analysis, conducted with the lavaan package (Rosseel, 2012) in R, to assess how root biomass and other measured soil factors

interact to affect observed EPSac content and the percentage of water-stable aggregates. Although path analysis is built for larger sample sizes than we have in our study, it provides conservative fit estimates when applied to small samples (Shipley, 2016). Using a workflow based on that presented by Petersen et al. (2012), we developed a full model of interacting paths between root biomass, soil water potential, pH, microbial biomass, DOC, DN, PO_4 accumulation, EPSac content, and the percentage of water-stable aggregates, based on theoretical linkages between the relevant measured variables (Fig. S4). We iteratively removed non-significant edges between the measured soil factors ($p < 0.1$) from the resulting path model until all edges were significant, and evaluated the fit of this reduced model to the data using a $\mathbf{X}^2$ test and the Tucker-Lewis Index. Visualization of the resulting path analysis was performed using the *semPlot* package (Epskamp, 2019) in R.

3. Results

3.1. EPSac and soil factors

EPSac concentrations in mesocosm soils after 143 days of SG growth varied significantly as a function of both treatment (ANOVA, $F = 5.16$, D.F. $= 4$, $P = 0.001$) and depth (ANOVA, $F = 238$, D.F. $= 2$, $P < 0.001$;

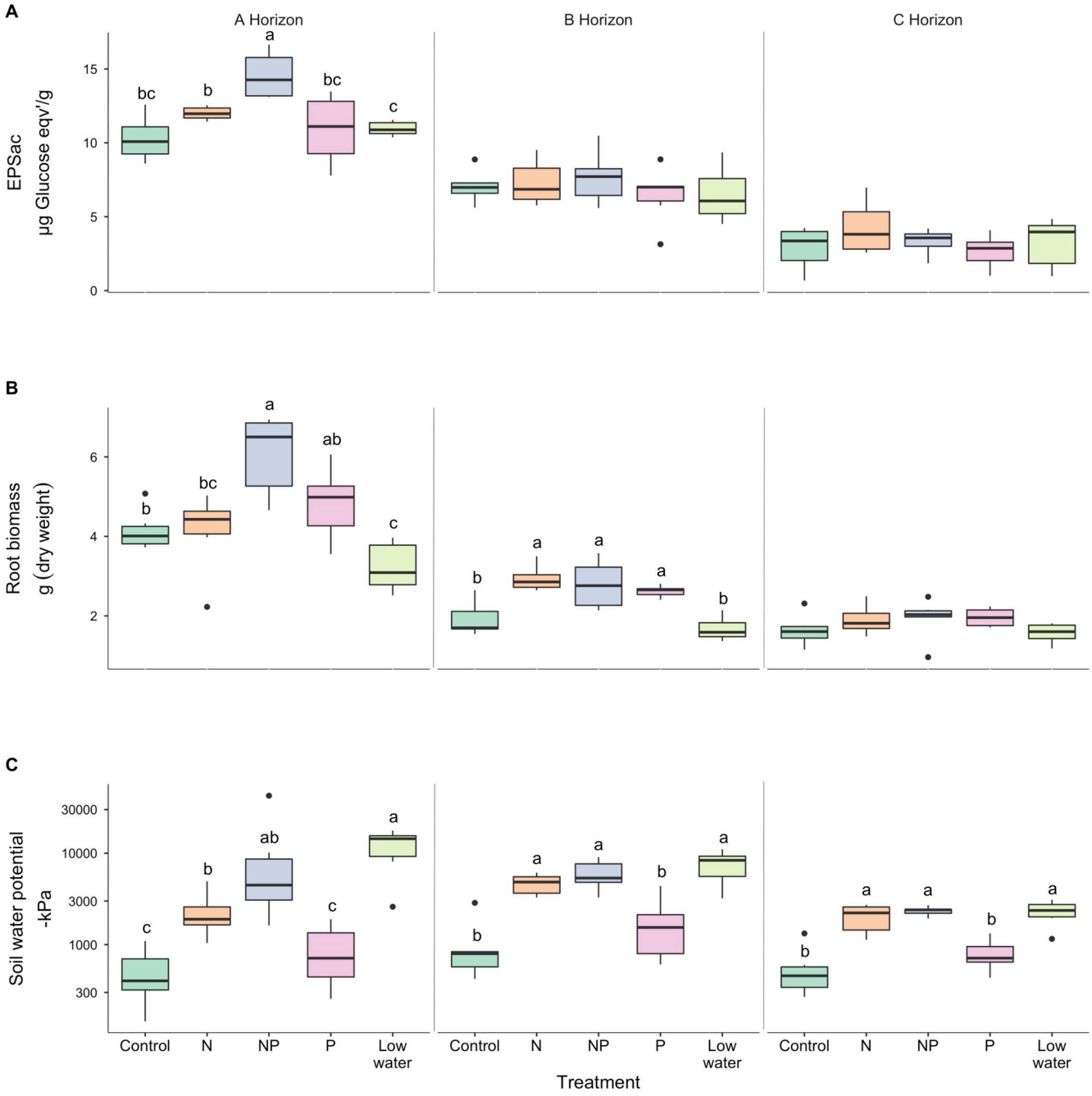

Fig. 1. EPSac and root biomass in switchgrass (SG) microcosms with five fertilizer/moisture treatments and three soil horizons after 140 days of growth. Box-whisker plots of A) EPSac content (glucose equivalent, micrograms per gram dry soil), B) SG root biomass (grams dry weight) recovered from bulk soil by treatment and horizon, and C) soil water potential (negative kilopascals) converted from gravimetric water content using moisture release curves developed for each horizon and log-transformed. Lowercase letters indicate significant differences between treatments within a horizon (Welch's *t*-test $P < 0.05$, after Benjamini-Hochberg correction for multiple testing). $n = 6$ per treatment/horizon.

Fig. 1A). In all treatments, EPSac content was greatest in the surface A horizon; ranging from 11.74 ± 2.04 μg g^{-1} (mean ± SD) in the A horizon to 6.99 ± 1.60 μg g^{-1} and 2.28 ± 1.43 μg g^{-1} in the B and C horizons, respectively (Fig. 1A). EPSac content only differed between treatments in the A horizon (ANOVA, F = 8.24, D.F. = 4, P < 0.001; Fig. 1A), and these differences were primarily driven by the enhanced EPSac content observed in the +NP treatment relative to all other treatments (Welch's t-tests, P < 0.025).

Root biomass exhibited similar trends as EPSac - the greatest root biomass was observed in the A horizon, with reduced biomass in the B and C horizons (Fig. 1B). Root biomass varied significantly by treatment in the A horizon (ANOVA, F = 9.64, D.F. = 4, P < 0.001; Fig. 1B), and was highest in the +NP treatment. Root biomass also varied significantly by treatment in the B horizon (ANOVA, F = 12.36, D.F. = 4, P < 0.001; Fig. 1B), mostly as a result of higher root biomass observed in fertilized treatments.

In all three soil horizons, soil water potential (measured at the time of the destructive harvest) was significantly lower in both N-fertilized treatments and the low-watering regime treatment relative to the control and +P treatments (Fig. 1C). Continuous soil water potential measurements from the A horizon of control and low water mesocosms for the 12 days of CO_2 labeling showed diurnal variation in soil water potentials was increased in drier soils (Fig. S5).

DOC exhibited similar trends as both EPSac and root biomass: DOC was highest and varied significantly between treatments in the A horizon; it was also significantly higher in the N and +NP treatments relative to all the others (Welch's t-tests, P < 0.019) (Table 1). DN was significantly higher in the A and B horizon of both nitrogen-amended treatments. DN was also significantly higher in the +N treatment relative to the +NP treatment, possibly indicating greater demand for N in the higher root biomass + NP treatment (Table 1). Accordingly, N fertilized treatments had the lowest ratios of DOC to DN (dissolved C/N, Table 1). In the A horizon, the +N and +NP treatments had significantly lower pH than non-N treatments (Table 1).

PLFA-measured microbial biomass was significantly affected by soil depth, with minimal biomass in the B horizon and barely detectable biomass in the C horizon (F = 349, D.F. = 1, P < 0.001). We did not observe significant treatment effects on microbial biomass across horizons (F = 2.43, D.F. = 4, P = 0.065; Table 1) or within the surface horizon (F = 1.03, D.F. = 4, P = 0.414).

We compared the influence of measured soil properties on EPSac across all treatments and horizons using multiple linear regression. Many factors were significantly correlated with one another (Fig. S2, S3); the most collinear factors were removed from the analysis according to their VIF (as explained in the Methods section). The resulting model explains a large proportion of the variation in EPSac (R^2 = 0.799) between treatments and horizons; root biomass, soil water potential, DN and microbial biomass were the most significant explanatory factors (P = 0.010, 0.034, 0.010 and < 0.001, respectively; Table 2). Because our dependent variable, EPSac, only varied significantly between treatments in the A horizon, we did not investigate interactions between treatment and depth in other variables, and we employed a second model for only the A horizon. This model also succeeded in capturing most of the variability in observed EPSac between treatments (R^2 = 0.667); root biomass was again the most significant factor (P < 0.001), and soil water potential and pH were additional significant factors (P = 0.007 and 0.009, respectively). A final model was developed with N addition included as a confounding factor to account for decreases in pH as a result of N fertilization (Table 1). In this model root biomass and soil water potential were the most significant factors controlling EPSac (P < 0.001 and P = 0.017, respectively), and pH was no longer significant (P = 0.198).

3.2. ^{13}C-labeled EPSac and total soil carbon

To assess the proportion of total soil C that was EPSac, we expressed soil EPSac content as a fraction of total soil C. We found ~0.3% of soil carbon is EPSac, with no significant differences between treatments and horizons. Dividing the ^{13}C-EPSac by the total ^{13}C found in the bulk soil (Table S1) revealed that 0.18% of newly-fixed plant-derived C had been assimilated into EPSac. There were no significant differences in the proportion of freshly fixed C recovered in EPSac between treatments. We obtained this data only for the A horizon, as a substantial amount of soil was needed to extract sufficient EPSac for ^{13}C IRMS analysis and significant differences in EPSac content were not found between treatments in the B and C horizon.

3.3. EPSac monosaccharide composition

We analyzed the monosaccharide composition of soil EPSac in the A horizon to assess its potential origin by calculating the ratios of recovered galactose + mannose (G + M, microbially derived) to arabinose + xylose (A + X, plant derived). This ratio was consistently above the accepted cutoff of 2.00 in our samples (average of 3.92 ± 0.25),

Table 1
Soil chemical properties (by soil horizon) in Panicum virgatum (switchgrass) mesocosms grown with five different nutrient/water treatments.

Horizon	Treatment	DOC[a] μg g^{-1}	DN[b] μg g^{-1}	Dissolved C/N	pH	Microbial biomass ng PLFA g^{-1}
A	Control	26.5 ± 1.6 b*	3.2 ± 0.2 c	8.3 ± 0.4 a	5.27 ± 0.12 a	10.3 ± 1.5
	+N	30.3 ± 1.8 a	21.4 ± 3.3 a	1.4 ± 0.2 d	4.94 ± 0.13 b	9.0 ± 0.4
	+NP	32.4 ± 1.8 a	12.3 ± 3.0 b	2.8 ± 0.8 c	4.96 ± 0.14 b	9.7 ± 1.7
	+P	25.7 ± 2.1 b	3.4 ± 0.2 c	7.5 ± 0.5 b	5.31 ± 0.15 a	9.8 ± 1.0
	Low water	24.9 ± 3.5 b	3.3 ± 0.4 c	7.6 ± 0.8 ab	5.33 ± 0.07 a	10.2 ± 1.4
B	Control	17.9 ± 2.6 ab	2.5 ± 2.0 b	9.3 ± 3.2 a	6.2 ± 0.08 ab	4.3 ± 0.4
	+N	17.9 ± 1.6 b	9.5 ± 5.9 ab	2.5 ± 1.4 b	6.25 ± 0.09 a	3.0 ± 0.3
	+NP	22.0 ± 4.6 ab	7.0 ± 1.2 a	3.2 ± 0.8 b	6.25 ± 0.04 a	4.0 ± 0.7
	+P	18.8 ± 2.6 ab	2.0 ± 0.4 b	9.7 ± 1.1 a	6.11 ± 0.07 b	3.5 ± 0.1
	Low water	21.7 ± 0.9 a	2.4 ± 0.4 b	9.2 ± 1.3 a	6.09 ± 0.07 b	3.2 ± 0.9
C	Control	17.2 ± 2.2	1.4 ± 0.6	15.2 ± 7.0 ab	6.47 ± 0.16	2.1 ± NA
	+N	16.7 ± 1.5	1.4 ± 0.3	12.4 ± 2.8 a	6.46 ± 0.08	1.9 ± 0.4
	+NP	17.0 ± 2.7	2.6 ± 0.5	6.9 ± 1.6 b	6.43 ± 0.07	2.2 ± 0.3
	+P	17.7 ± 5.0	1.5 ± 0.8	14.7 ± 6.0 ab	6.4 ± 0.12	NA ± NA
	Low water	18.6 ± 2.8	1.5 ± 0.5	13.2 ± 3.1 a	6.4 ± 0.13	1.8 ± NA

* Lowercase letters indicate significant differences between treatments within a horizon (Welch's *t*-test P < 0.05, after Benjamini-Hochberg correction for multiple testing). Means ± SD, n = 6 per treatment/horizon.

[a] Dissolved organic carbon.

[b] Dissolved nitrogen.

Table 2
Multiple linear regression models describing relations between most highly explanatory soil factors and EPS, after removing collinear explanatory soil factors with variance inflation factor values above 3 (Zuur et al., 2010).

Factor			Root biomass		Soil water potential[a]		Dissolved nitrogen		Microbial biomass		pH	
Model	Model R^2	Model P	β[b]	P	β	P	β	P	β	P	β	P
All horizons	**0.799**	**<0.001**	**0.676**	**0.010**	**0.973**	**0.034**	**0.102**	**0.011**	**0.631**	**<0.001**	–	–
A horizon	**0.667**	**<0.001**	**1.001**	**<0.001**	**1.038**	**0.007**	–	–	–	–	**−3.087**	**0.009**
A horizon; Controlled for N treatments	**0.655**	**<0.001**	**0.977**	**<0.001**	**0.995**	**0.0170**	–	–	–	–	−2.611	0.198

[a] Absolute value soil water potential units.
[b] Factor specific slope when other factors are constant.

indicating EPSac had a likely microbial origin (Chenu, 1995; Gunina and Kuzyakov, 2015; Oades, 1984). The observed ratio was significantly lower in the A horizon of the +NP, +N and low-watering regime treatments relative to the control and +P treatments ((3.78 ± 0.19, mean ± SD across treatments) vs. (4.14 ± 0.15), respectively; $P < 0.02$) (Table S2). Given that SG root mucilage itself appears to have high galactose content (resulting in a (G + M)/(A + X) ratio of 1.45 ± 0.17), we also employed a more conservative M/(A + X) ratio to confirm that the majority of the EPSac we extracted was most likely microbial in origin. Recovered EPSac still had a value above 2.00 with this modified ratio (2.24 ± 0.13, on average), giving us confidence in our prior conclusion. This more conservative ratio did not differ between treatments in the A horizon. EPSac monosaccharide composition was found to vary significantly as a result of treatment (MANOVA $F = 6.34$, D.F. = 20, $P < 0.001$).

3.4. Soil aggregate stability and relationship to measured variables

We measured the percentage of aggregates that were water-stable to assess the effects of treatment and EPSac content on soil aggregation. The percentage of water-stable aggregates was significantly higher in the +NP treatment (Fig. 2), and we measured a significant positive correlation between soil EPSac and the percentage of water stable aggregates (Pearson $R = 0.44$, $P = 0.017$; Fig. S3).

We conducted path analysis to determine how root biomass and our observed soil characteristics may interact to impact both EPSac content and the percentage of water-stable aggregates in our mesocosms. Our full model (including all of the soil variables measured) fit the data well according to the model chi-squared statistic ($\mathbf{X}^2 = 5.474$, D.F. = 4, P = 0.242), as did the reduced model in which we removed non-significant edges ($\mathbf{X}^2 = 14.066$, D.F. = 21, P = 0.867). The Tucker-Lewis index, which is more sensitive to the number of parameters included in the analysis, indicated that our reduced model fit the data very well (TLI = 1.105, above the 0.9 threshold), which is particularly notable given that TLI is vulnerable to incorrectly assessing a poor model fit when sample sizes are small (Hu and Bentler, 1999). Given that the reduced model is a nested variant of the full model, we verified that the reduced model did not fit the data in a significantly different manner from the full model using a maximum likelihood ratio test ($\mathbf{X}^2$ difference = 8.592, D.F. = 17, $P = 0.952$). The reduced model shows that root biomass affects soil EPSac content both directly and through the DOC pool, whereas soil water potential acts separately on both EPSac and the percentage of water-stable aggregates (Fig. 3). Soil aggregation is also affected by pH, though our multiple linear regression analyses indicate this is likely an artifact of our N addition treatment. In addition, EPSac and water-stable aggregates co-vary positively with one another.

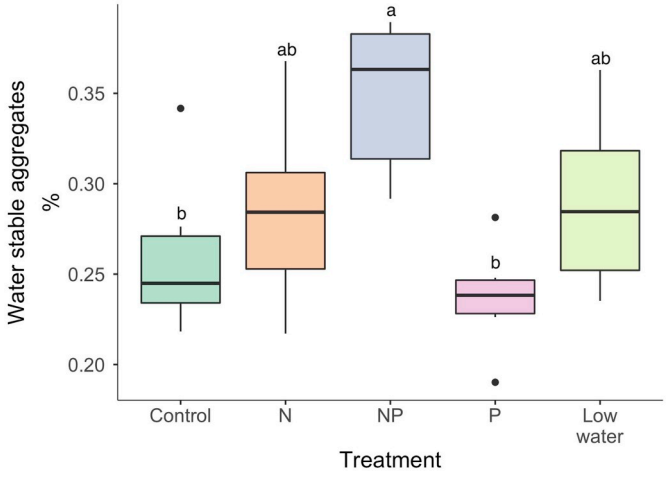

Fig. 2. Soil aggregate stability in the surface horizon of switchgrass (SG) mesocosms with five fertilizer/moisture treatments after 140 days of growth. Box-whisker plot of the percentage of aggregates recovered from bulk soil that were water-stable in the A horizon. Lowercase letters indicate significant differences between treatments (Welch's *t*-test $P < 0.05$, after Benjamini-Hochberg correction for multiple testing). n = 6 per treatment.

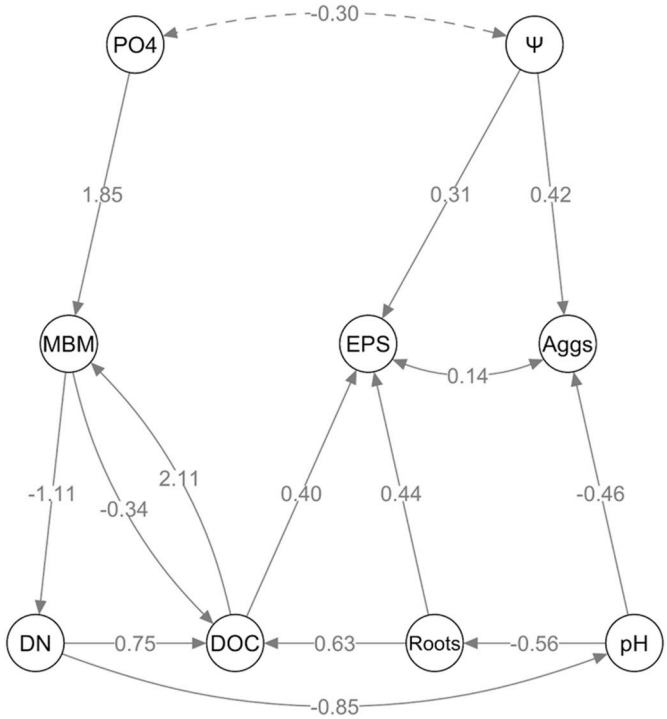

Fig. 3. Path analysis of soil factors affecting EPSac and soil aggregate stability in the surface soil horizon of SG mesocosms with five fertilizer/moisture treatments after 140 days of growth in a 'reduced model', where only significant edges ($P < 0.05$) are retained. Node labels correspond to the following measured variables: EPSac content (EPS), frequency of water-stable aggregates (Aggs), soil water potential (Ψ), pH, SG root biomass (Roots), dissolved organic carbon (DOC), total dissolved nitrogen (DN), microbial biomass measured by PLFA (MBM), and phosphate accumulation on anion exchange membranes over the course of the study (PO4).

3.5. EPSac in soil core field sampling

Significantly larger stocks of EPSac were observed in long-term SG field soils compared to those measured in paired annual cultivated fields, under rye (Red River) or wheat and sorghum (Stillwater) grown with consistent tillage (Red River $F = 33.33$, D.F. $= 1$, $P < 0.001$; Stillwater $F = 40.12$, D.F. $= 1$, $P < 0.001$; Fig. 4). This significant enhancement of EPSac content extended over 1.5 m deep in the soil, with concentrations of ~10 μg g^{-1} in the surface layers and ~2 μg g^{-1} below 180 cm depth soil samples (Red River $F = 2.46$, D.F. $= 4$, $P = 0.062$; Stillwater $F = 4.43$, D.F. $= 4$, $P = 0.005$; Fig. 4).

4. Discussion

4.1. Nutrient and water treatment effects on switchgrass root biomass and EPSac

Our results demonstrate that when SG is cultivated in marginal soils, root biomass and rhizodeposition are important drivers of soil EPSac content. In support of our hypothesis, water stress was a significant driver of soil EPSac content, and the EPSac produced under water stress may have enhanced water-stable soil aggregation. However, our results did not support our hypothesis that soil microbes exposed to greater nutrient limitation would produce more EPSac. Most studies indicating that high C:N ratios enhanced EPSac production (Pal and Paul, 2013; Roberson, 1991; Sheng et al., 2006; Wang and Yu, 2007) were performed with microbial isolates in culture. Data regarding microbial EPSac production in response to N or P limitation in soil is scarce, though it has been shown that specific N management practices can increase or decrease the quantity of EPSac-like carbohydrates bound to the soil heavy fraction, depending on the quantity of N added (Roberson et al., 1995).

Notably, Redmile-Gordon et al. recently showed that high C availability can increase soil EPSac content (2015). This suggests that the availability of C precursors for EPSac production may be a limiting factor in soil environments, a condition that is likely important in marginal soils with low organic C stocks. Zhalnina et al. (2018) linked exudate chemistry of an annual grass to the presence of bacterial taxa in its rhizosphere capable of degrading said exudates, indicating that C compounds exuded into the rhizosphere exert strong control on rhizosphere microbes. In our study, DOC concentrations were higher in treatments with high root biomass and EPSac, suggesting that enhanced root biomass may have provided C precursor compounds to the soil microbiota. Our path analysis also provides support for this hypothesis. While our measurements of DOC and EPSac may overlap to some extent, our EPSac extraction method targets polymeric carbohydrates bound within the soil matrix (Wang et al., 2019), whereas our DOC assay targets soluble C compounds.

Several field studies suggest that SG productivity is relatively insensitive to N-fertilization (Brejda, 2000; Pedroso et al., 2011), and Thomason et al. (2005) notably observed that SG grown in an Oklahoma sandy loam with no N amendment had nearly as much biomass as plants grown with significant (>400 kg ha^{-1} $year^{-1}$) N fertilization. However, SG root biomass clearly responded to the +NP treatment in our greenhouse mesocosm study. This is likely due to the highly N- and P-deplete character of the marginal soil used in our experiment. The literature suggests there are threshold values of N availability below which N amendment can enhance SG biomass (Brejda, 2000), and local advisory agencies in Oklahoma recommend that farmers provide N fertilizer when initially sowing SG (Arnall et al., 2018). Thomason et al. (2005) also found evidence for P-limitation of SG biomass under N fertilization in their study, and P-limitation may have played a role in the lack of SG biomass response to our N-only amendment – we observed a higher increase in root biomass in our + NP treatment relative to the +N treatment, and higher levels of dissolved N consumption in the +NP treatment.

Root biomass may also alter EPSac production by reducing soil water potential and increasing its diurnal variability (Caldwell et al., 1998; Kirkham, 2005) such that microbial EPSac production may have been promoted by increased water stress (Roberson and Firestone, 1992). Indeed, the only other significant predictor for EPSac production in the A horizon was soil water potential. The role of EPSac in enhancing microbial resistance to low water potential has been extensively discussed in the literature (Costa et al., 2018; Schimel, 2018), with most data derived from studies on isolates (Chang et al., 2007; Roberson and Firestone, 1992). In our study, soil water potential was significantly correlated with EPSac content, in a manner consistent with previous research on the effects of water stress on microbial EPSac production (Roberson and Firestone, 1992; Sandhya and Ali, 2015). Furthermore, a recent study of soil EPSac accumulation found that EPSac production was reduced in plots that received more water (Marchus et al., 2018); when plant cover was removed from wetter plots, less EPSac was

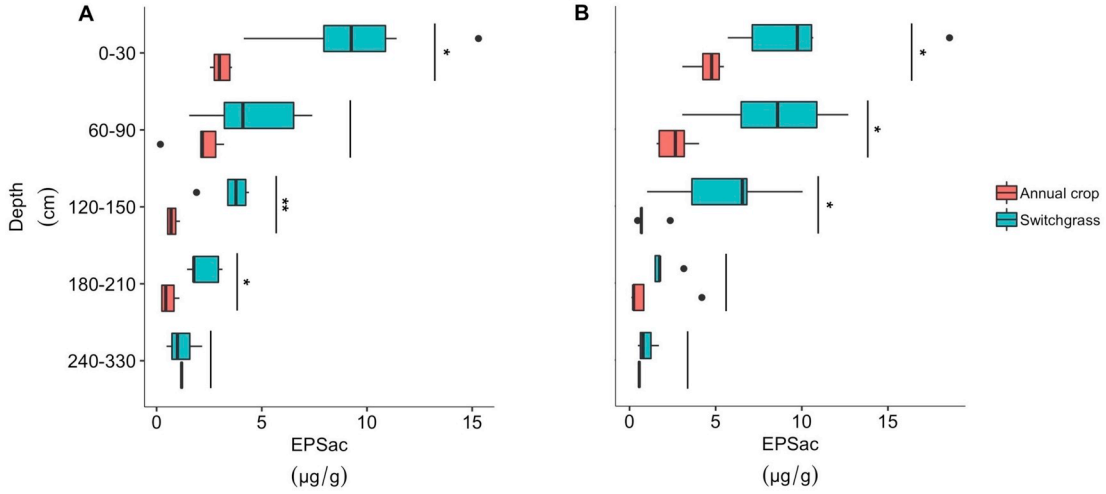

Fig. 4. Soil depth profile of EPSac content in switchgrass (SG) and annual crop fields. Box-whisker plots of EPSac content (glucose equivalent micrograms per gram dry soil) in deep soil cores from plots subjected to A) 20-year (Stillwater, OK) and B) 10-year (Red River site, OK) no-till cultivation of deep-rooted SG compared to paired plots at each site planted with short-rooted annual rye or wheat/sorghum and managed with conventional tillage. Asterisks indicate significant differences between SG plots compared to paired annual crop plots at each sampled depth (Welch's *t*-test, $P < 0.05$ for * and <0.01 for **, after Benjamini-Hochberg correction for multiple testing). n = 6.

observed. It is well known that actively evapotranspiring plants with dense root systems can cause daily changes in soil water potential (Caldwell et al., 1998; Kirkham, 2005). Continuous soil water potential measurements from our control and low water treatments show that plants enhanced water stress in bulk soil during the day in a manner that was exacerbated in drier soils.

4.2. Quantifying soil EPSac and validating its microbial origin

The quantity of EPSac we recovered is relatively low compared to some previous studies – for instance, in a recent watering manipulation experiment in an annual grassland, significantly higher amounts of EPSac were recovered (150–300 μg g^{-1}) using a hot-water extraction method (Marchus et al., 2018). Significantly higher EPSac content (170–460 μg g^{-1}) was also found in another annual grassland soil using the a similar CER extraction method (Redmile-Gordon et al., 2014). Thus, our choice of extraction method is not likely the cause of our lower EPSac values. We suspect that the low microbial biomass, very low total carbon content and low availability of DOC in our marginal soil likely constrained the amount of EPSac that could be produced by local microbial communities. Our EPSac results are not markedly different from those of Marchus et al. (2018) once adjusting for total soil C, and taking the higher microbial biomass they observed (~200–300 μg C g^{-1}) in comparison to our study (~70 μg C g^{-1}) into account after converting to similar units (Bailey et al., 2002). Notably, that study also found significant correlation between microbial biomass and EPSac content (Marchus et al., 2018). Carbohydrate content and microbial biomass vary extensively across soil types; while our soils have low microbial biomass and EPSac content, our observed values do fall well within the wide range found in a study of 108 arable, grassland, and forest soils (Joergensen et al., 1996).

In our study, recovered EPSac had a distinctly microbial signature, even though the microbial biomass pool we measured was relatively small and non-responsive. However, microbial biomass can be insensitive over seasonal time scales in grasslands (Waldrop and Firestone, 2006) and can cycle more carbon than is contained in standing biomass over time (Potthoff et al., 2008). Unfortunately, we were unable to determine the monosaccharide signature of EPSac produced in the absence of growing SG plants, because of a design flaw in our no-plant control mesocosms. This is an oversight that a future study would do well to address.

4.3. Soil aggregate stability controlled by same factors as EPSac production

Soil aggregate stability has been previously linked to SG cultivation. For example, Tiemann and Grandy (2015) found that planting SG significantly enhanced the amount and stability of aggregates in a sandy loam after four years. Similarly, McGowan et al. (2019) specifically linked aggregation to SG roots, by quantifying aggregation and root biomass in seven different cropping systems including SG. They established that both aggregation and root biomass were enhanced under SG relative to annual row crops under no-till management after seven years. This finding mirrors that of Ontl et al. (2015), who found that aggregation and root biomass were both enhanced under SG cultivation relative to annual row crops under no-till management after three years. There is also significant evidence that perennial grasslands, in general, have enhanced soil aggregation rates (Chimento et al., 2016; McLauchlan et al., 2006). O'Brien and Jastrow (2013) drew on a long-term (>20 years) chronosequence of restored tallgrass prairie to establish that not only is aggregation significantly increased under restored perennial grasslands relative to annual cropland, the mechanism for enhanced aggregation appears to be a greater abundance of free microaggregates. Notably, the adhesive properties of EPSac are hypothesized to play a significant role in the initial formation of microaggregates (Six et al., 2000).

Dense root systems—such as those under perennial grasslands—may also enhance the wetting and drying cycles of soil (as they did in our study), a process that can enhance aggregate stability depending on the type of clays present (Singer et al., 1992). Our results suggest that roots and rhizodeposition control the soil conditions which regulate both microbial EPSac production and aggregate stability. This result is in-line with the findings and conceptual model presented by Baumert et al. (2018), who suggest that soil aggregation in the presence of root exudates can be controlled by interactions between soil water content and the microbial production of "gluing agents". We are not aware of any other studies showing a significant effect of SG cultivation on soil aggregate stability in <1 year, with the distinction that our results were obtained in a greenhouse. We also note these results contrast with a previous finding that SG grown under similar N fertilization rates (67 kg ha^{-1}) did not exhibit enhanced root biomass or soil aggregation relative to controls (Jung et al., 2011); however, that study was performed on a silt loam with significantly higher C and N content than the sandy loam we used.

Many factors may play a role in the promotion of stable soil aggregates. Our path analysis indicates that root biomass exerts strong control over EPSac content by providing C to microbes through the DOC pool, while soil water potential exerts direct control over both EPSac content and aggregate stability. Furthermore, a mechanistic connection between aggregate stability and EPSac content (which co-vary in our study) seems likely, given that EPSac is thought to promote aggregate stability (Six et al., 2000; Six and Paustian, 2014). Further studies employing CER extractions of EPSac are required to determine if EPSac content and composition vary within different aggregate size classes relative to bulk soil, and within water-stable aggregates relative those that fragment. We found that EPSac monosaccharide composition varied between our treatments, but there is a need for future studies that quantitatively (i.e., using mass spectrometry or nuclear magnetic resonance) investigate how differences in EPSac composition can affect the formation of water-stable aggregates.

While path analysis cannot establish causal relationships (Shipley et al., 2016), it is a useful tool for generating mechanistic hypotheses that can later be tested in ecological experiments. For example, Jastrow et al. (1998) used path analysis to determine linkages between root biomass, EPSac, soil OC, microbial biomass, fungal hyphae, and macroaggregation in a restored tallgrass prairie chronosequence, and found that root biomass and fungal hyphae were the strongest contributing factors to the enhanced aggregation they observed – not EPSac. However, their study assessed EPSac content through hot-water extraction, which can bias observations as a result of cell lysis (Wang et al., 2019), and therefore it is possible that CER-extracted EPSac would tell a different story. Jastrow et al. did find that root biomass exerted strong control on the EPSac pool in their study, which we also observed. We did not assess fungal biomass in our study, and future studies investigating the effects of SG cultivation on EPSac content or aggregation should employ assays of fungal activity – particularly of arbuscular mycorrhizal fungi, whose biomass has recently been linked to macroaggregation under SG cultivation in the field (McGowan et al., 2019).

4.4. Carbon flow from plant photosynthate into microbial EPSac

The EPSac fraction of the soil C pool responded to our treatments and may exert some control over the formation of water-stable aggregates, highlighting the importance of assessing EPSac stocks in soils. This may be particularly true in marginal soils, where the overall depletion of organic C in the surrounding soil environment may enhance the effect of a small pool of actively synthesized polysaccharides that can alter soil characteristics and microbial viability (Wolfaardt et al., 1999). Using a $^{13}CO_2$ tracer allowed us to track carbon flow from plant photosynthate into microbial EPSac. The percent of the total soil ^{13}C that was in in EPSac C was ~0.18%. This percentage indicates how much of the recently fixed C exuded from the roots and still present in the soil was

incorporated into EPSac by soil microorganisms during the 12 days of labeling at the end of the plant growth period. We expected this number to perhaps be higher given that the availability of plant C appears to control microbial EPSac production. However, labeling at a more photosynthetically active period of plant phenology could produce significantly different results.

To our knowledge, no other study has examined the fraction of EPSac produced using freshly fixed plant photosynthate, making it difficult to place our results in context. Future experiments taking advantage of isotope-enabled approaches and labeling systems that have emerged during the last decade (Pett-Ridge and Firestone, 2017) will enable us to evaluate the magnitude of this fraction and how this aspect of plant-microbe interaction may vary between plant species, soil types and abiotic stress conditions. For instance, studies that directly quantify plant photosynthetic rates during labeling could determine the partitioning of plant photosynthate into root exudates and the amount processed by microbial communities into EPSac. Future studies could also compare bulk versus rhizosphere soil EPSac content, monosaccharide composition, or the frequency of water-stable aggregates.

4.5. Higher EPSac in SG fields than adjacent annual grass fields

Our greenhouse study establishes that SG cultivation can alter soil EPSac stocks over less than one growing season, but we are not aware of studies that have assessed EPSac after SG cultivation in the field. Ma et al. (2000) showed that ten years of SG cultivation with similar rates of N amendment (112 kg ha^{-1}) resulted in significantly enhanced soil organic C from 0 to 15 cm and from 15 to 30 cm in an Alabama sandy loam, and several other studies have further established that soil organic C is enhanced under long-term SG cultivation when compared to paired annual crop fields (Chimento et al., 2016; Dou et al., 2013; McGowan et al., 2019). Our field results clearly indicate that SG cultivation enhances stocks of EPSac more than a meter deep within the soil profile. Root density was also significantly enhanced down to at least 30 cm deep under SG compared to annual crops (data not shown). This indicates that increased EPSac under SG cultivation could be implicated in the increased soil aggregation observed in field soils under perennial grass cultivation. Enhanced aggregation could then provide a mechanism for the persistence of C under SG cultivation (Liao et al., 2006; McGowan et al., 2019). While the overall sustainability of SG cultivation is a function of many agricultural ecosystem characteristics (trace gas production, fertilization and associated N and P loss to water systems, etc.), the long-term impacts on soil C retention and soil structure are important indices of ecosystem sustainability.

5. Conclusions

We found that SG cultivation can enhance microbial EPSac production in a marginal soil. We hypothesize that SG root biomass enhances the availability of organic C compounds, providing precursors for microbial EPSac production. Root biomass and soil water potential combine to exert significant control over microbial EPSac production as well as water-stable aggregate formation. Growing roots absorb water from the soil, increasing water stress and thereby indirectly enhancing microbial EPSac production and water-stable aggregation formation. We also found evidence of significantly enhanced EPSac stocks in two long-term SG field plots, suggesting that these mechanisms may be broadly relevant. More research is required to determine how microbial communities under SG process rhizodeposits into EPSac and how this EPSac translates to beneficial soil characteristics such as aggregate formation. Broader scale field-studies will be needed to assess the rates and importance of EPSac accumulation under relevant land management practices.

Acknowledgments

This research is based upon work supported by the U.S. Department of Energy Office of Science, award DE-SC0014079 to UC Berkeley and subcontracts to the Noble Research Institute, the University of Oklahoma and Lawrence Livermore National Laboratory (award SCW1555). Work at LLNL was conducted under the auspices of DOE Contract DE-AC52-07NA27344. YS was supported by postdoctoral fellowship grant no. 2016-67012-24717 from the USDA National Institute of Food and Agriculture. We thank David Orme for allowing us to collect soil from his ranch in Anadarko Oklahoma, and Hugh Aljoe, Kelly Craven and Shawn Norton for facilitating site access and soil collection. We thank Yanqi Wu for the opportunity to sample Oklahoma State University's field site near Stillwater, OK. The custom $^{13}CO_2$ labeling system was designed by Don Herman. Thanks also to Katerina Estera-Molina, Anne Kakouridis, Sarah Baker, Steve Blazewicz, Evan Starr, Ka Ki Law, Mengting Yuan, Heejung Cho, Alexa Nicholas, Eoin Brodie, Peter Nico, Caleb Herman, Ashley Campbell, and Amrita Bhattacharyya for their help with the destructive harvest of mesocosms; Yuan Wang, Na Ding, Travis Simmons, Josh Barbour, Mellisa McMahon, Jialiang Kuang, Colin Bates, Ryan Gini and Noah Sokol for their help with deep core soil sampling; Madeline Moore, David Sanchez, Cynthia-Jeanette Mancilla and Ilexis Jacoby for their help with processing and soil chemical analyses; and Trent Northen and Kate Zhalnina for their help with TOC/TN analysis.

Appendix A. Supplementary data

Supplementary data related to this article can be found at https://doi.org/10.1016/j.soilbio.2020.107742.

References

Seki, K., 2007. SWRC fit – a nonlinear fitting program with a water retention curve for soils having unimodal and bimodal pore structure. Hydrology and Earth System Sciences Discussions 4, 407–437. https://doi.org/10.5194/hessd-4-407-2007.

Abraha, M., Gelfand, I., Hamilton, S.K., Chen, J., Robertson, G.P., 2019. Carbon debt of field-scale conservation reserve program grasslands converted to annual and perennial bioenergy crops. Environmental Research Letters 14, 024019. https://doi.org/10.1088/1748-9326/aafc10.

Adessi, A., Cruz, R., Carvalho, D., Philippis, R.D., Branquinho, C., Marques da Silva, J., 2018. Microbial extracellular polymeric substances improve water retention in dryland biological soil crusts. Soil Biology and Biochemistry 116, 67–69. https://doi.org/10.1016/j.soilbio.2017.10.002.

Ali, SkZ., Sandhya, V., Grover, M., Kishore, N., Rao, L.V., Venkateswarlu, B., 2009. Pseudomonas sp. strain AKM-P6 enhances tolerance of sorghum seedlings to elevated temperatures. Biology and Fertility of Soils 46, 45–55. https://doi.org/10.1007/s00374-009-0404-9.

Amellal, N., Bartoli, F., Villemin, G., Talouizte, A., Heulin, T., 1999. Effects of inoculation of EPS-producing Pantoea agglomerans on wheat rhizosphere aggregation. Plant and Soil 211, 93–101. https://doi.org/10.1023/A:1004403009353.

Anderson-Teixeira, K.J., Davis, S.C., Masters, M.D., Delucia, E.H., 2009. Changes in soil organic carbon under biofuel crops. GCB Bioenergy 1, 75–96. https://doi.org/10.1111/j.1757-1707.2008.01001.x.

Arnall, B., Jones, J., Pugh, B., Rocateli, A., Sanders, H., Warren, J., Zhang, H., 2018. Oklahoma Forage and Pasture Fertility Guide. Oklahoma State University, Stillwater, OK.

Bailey, V.L., Peacock, A.D., Smith, J.L., Bolton, H., 2002. Relationships between soil microbial biomass determined by chloroform fumigation–extraction, substrate-induced respiration, and phospholipid fatty acid analysis. Soil Biology and Biochemistry 34, 1385–1389. https://doi.org/10.1016/S0038-0717(02)00070-6.

Baumert, V.L., Vasilyeva, N.A., Vladimirov, A.A., Meier, I.C., Kögel-Knabner, I., Mueller, C.W., 2018. Root exudates induce soil macroaggregation facilitated by fungi in subsoil. Frontiers in Environmental Science 6, 1–17. https://doi.org/10.3389/fenvs.2018.00140.

Benjamini, Y., Hochberg, Y., 1995. Controlling the false discovery rate: a practical and powerful approach to multiple testing. Journal of the Royal Statistical Society: Series B 57, 289–300. https://doi.org/10.1111/j.2517-6161.1995.tb02031.x.

Brejda, J.J., 2000. Fertilization of native warm-season grasses. In: Native Warm-Season Grasses: Research Trends and Issues, CSSA Special Publication. Crop Science Society of America and American Society of Agronomy, Madison, WI, pp. 177–200. https://doi.org/10.2135/cssaspecpub30.c12.

Buyer, J.S., Sasser, M., 2012. High throughput phospholipid fatty acid analysis of soils. Applied Soil Ecology 61, 127–130. https://doi.org/10.1016/j.apsoil.2012.06.005.

Caldwell, M.M., Dawson, T.E., Richards, J.H., 1998. Hydraulic lift: consequences of water efflux from the roots of plants. Oecologia 113, 151–161. https://doi.org/10.1007/s004420050363.

Celik, G.Y., Aslim, B., Beyatli, Y., 2008. Characterization and production of the exopolysaccharide (EPS) from Pseudomonas aeruginosa G1 and Pseudomonas putida G12 strains. Carbohydrate Polymers 73, 178–182. https://doi.org/10.1016/j.carbpol.2007.11.021.

Chang, W.-S., Mortel, M. van de, Nielsen, L., Guzman, G.N. de, Li, X., Halverson, L.J., 2007. Alginate production by Pseudomonas putida creates a hydrated microenvironment and contributes to biofilm architecture and stress tolerance under water-limiting conditions. Journal of Bacteriology 189, 8290–8299. https://doi.org/10.1128/JB.00727-07.

Chenu, C., 1995. Extracellular polysaccharides: an interface between microorganisms and soil constituents. In: Huang, P.M., Berthelin, J., Bollag, J.-M., McGill, W.B. (Eds.), Environmental Impacts of Soil Component Interactions: Land Quality, Natural and Anthropogenic Organics, Volume I. Presented at the Impact of Interactions of Inorganic, Organic, and Microbiological Soil Components on Environmental Quality, pp. 217–233. Edmonton, Alberta, Canada.

Chenu, C., Cosentino, D., 2011. Microbial regulation of soil structural dynamics. In: Ritz, K., Young, I. (Eds.), The Architecture and Biology of Soils: Life in Inner Space. CABI, Wallingford, pp. 37–70. https://doi.org/10.1079/9781845935320.0037.

Chenu, C., Roberson, E.B., 1996. Diffusion of glucose in microbial extracellular polysaccharide as affected by water potential. Soil Biology and Biochemistry 28, 877–884. https://doi.org/10.1016/0038-0717(96)00070-3.

Cheshire, M.V., 1977. Origins and stability of soil polysaccharide. Journal of Soil Science 28, 1–10. https://doi.org/10.1111/j.1365-2389.1977.tb02290.x.

Chimento, C., Almagro, M., Amaducci, S., 2016. Carbon sequestration potential in perennial bioenergy crops: the importance of organic matter inputs and its physical protection. GCB Bioenergy 8, 111–121. https://doi.org/10.1111/gcbb.12232.

Costa, O.Y.A., Raaijmakers, J.M., Kuramae, E.E., 2018. Microbial extracellular polymeric substances: ecological function and impact on soil aggregation. Frontiers in Microbiology 9. https://doi.org/10.3389/fmicb.2018.01636.

Dou, F.G., Hons, F.M., Ocumpaugh, W.R., Read, J.C., Hussey, M.A., Muir, J.P., 2013. Soil organic carbon pools under switchgrass grown as a bioenergy crop compared to other conventional crops. Pedosphere 23, 409–416. https://doi.org/10.1016/S1002-0160(13)60033-8.

DuBois, Michel, Gilles, K.A., Hamilton, J.K., Rebers, P.A., Smith, Fred, 1956. Colorimetric method for determination of sugars and related substances. Analytical Chemistry 28, 350–356. https://doi.org/10.1021/ac60111a017.

D'Angelo, E., Crutchfield, J., Vandiviere, M., 2001. Rapid, sensitive, microscale determination of phosphate in water and soil. Journal of Environmental Quality 30, 2206–2209. https://doi.org/10.2134/jeq2001.2206.

Epskamp, S., 2019. semPlot: Path Diagrams and Visual Analysis of Various SEM Packages' Output.

Fox, J., Weisberg, S., 2011. An R Companion to Applied Regression, second ed. SAGE Publications, Thousand Oaks, Calif.

Frølund, B., Palmgren, R., Keiding, K., Nielsen, P.H., 1996. Extraction of extracellular polymers from activated sludge using a cation exchange resin. Water Research 30, 1749–1758. https://doi.org/10.1016/0043-1354(95)00323-1.

Gelfand, I., Zenone, T., Jasrotia, P., Chen, J., Hamilton, S.K., Robertson, G.P., 2011. Carbon debt of Conservation Reserve Program (CRP) grasslands converted to bioenergy production. Proceedings of the National Academy of Sciences 108, 13864–13869. https://doi.org/10.1073/pnas.1017277108.

Gunina, A., Kuzyakov, Y., 2015. Sugars in soil and sweets for microorganisms: review of origin, content, composition and fate. Soil Biology and Biochemistry 90, 87–100. https://doi.org/10.1016/j.soilbio.2015.07.021.

Hu, L., Bentler, P.M., 1999. Cutoff criteria for fit indexes in covariance structure analysis: conventional criteria versus new alternatives. Structural Equation Modeling: A Multidisciplinary Journal 6 (1), 1–55. https://doi.org/10.1080/10705519909540118.

IUSS Working Group WRB, 2015. World Reference Base for Soil Resources 2014, Update 2015 International Soil Classification System for Naming Soils and Creating Legends for Soil Maps. World Soil Resources Reports No. 106. FAO, Rome.

Jackson, R.B., Mooney, H.A., Schulze, E.-D., 1997. A global budget for fine root biomass, surface area, and nutrient contents. Proceedings of the National Academy of Sciences 94, 7362–7366. https://doi.org/10.1073/pnas.94.14.7362.

Jastrow, J.D., Miller, R.M., Lussenhop, J., 1998. Contributions of interacting biological mechanisms to soil aggregate stabilization in restored prairie. Soil Biology and Biochemistry 30, 905–916. https://doi.org/10.1016/S0038-0717(97)00207-1.

Jastrow, J.D., Amonette, J.E., Bailey, V.L., 2007. Mechanisms controlling soil carbon turnover and their potential application for enhancing carbon sequestration. Climatic Change 80, 5–23. https://doi.org/10.1007/s10584-006-9178-3.

Jiao, Y., Cody, G.D., Harding, A.K., Wilmes, P., Schrenk, M., Wheeler, K.E., Banfield, J.F., Thelen, M.P., 2010. Characterization of extracellular polymeric substances from acidophilic microbial biofilms. Applied and Environmental Microbiology 76, 2916–2922. https://doi.org/10.1128/AEM.02289-09.

Joergensen, R.G., Mueller, T., Wolters, V., 1996. Total carbohydrates of the soil microbial biomass in 0.5 M K2SO4 soil extracts. Soil Biology and Biochemistry 28, 1147–1153. https://doi.org/10.1016/0038-0717(96)00111-3.

Jung, J.Y., Lal, R., Jastrow, J.D., Tyler, D.D., 2011. Nitrogenous fertilizer effects on soil structural properties under switchgrass. Agriculture, Ecosystems & Environment 141, 215–220. https://doi.org/10.1016/j.agee.2011.01.016.

Keiluweit, M., Bougoure, J.J., Nico, P.S., Pett-Ridge, J., Weber, P.K., Kleber, M., 2015. Mineral protection of soil carbon counteracted by root exudates. Nature Climate Change 5, 588–595. https://doi.org/10.1038/nclimate2580.

Kemper, W.D., Rosenau, R.C., 1986. Aggregate stability and size distribution. In: Methods of Soil Analysis, Part 1. Physical and Mineralogical Methods, second ed., pp. 425–442.

Kirkham, M.B., 2005. 19 - the ascent of water in plants. In: Kirkham, M.B. (Ed.), Principles of Soil and Plant Water Relations. Academic Press, Burlington, pp. 315–340. https://doi.org/10.1016/B978-012409751-3/50019-0.

Liang, C., Schimel, J.P., Jastrow, J.D., 2017. The importance of anabolism in microbial control over soil carbon storage. Nature Microbiology 2, 1–6. https://doi.org/10.1038/nmicrobiol.2017.105.

Liao, J.D., Boutton, T.W., Jastrow, J.D., 2006. Organic matter turnover in soil physical fractions following woody plant invasion of grassland: evidence from natural 13C and 15N. Soil Biology and Biochemistry, Ecosystems in Flux: Molecular and stable isotope Assessments of Soil Organic Matter Storage and Dynamics 38, 3197–3210. https://doi.org/10.1016/j.soilbio.2006.04.004.

Lützow, M.v., Kogel-Knabner, I., Ekschmitt, K., Matzner, E., Guggenberger, G., Marschner, B., Flessa, H., 2006. Stabilization of organic matter in temperate soils: mechanisms and their relevance under different soil conditions - a review. European Journal of Soil Science 57, 426–445. https://doi.org/10.1111/j.1365-2389.2006.00809.x.

Ma, Z., Wood, C.W., Bransby, D.I., 2000. Soil management impacts on soil carbon sequestration by switchgrass. Biomass and Bioenergy 18, 469–477. https://doi.org/10.1016/S0961-9534(00)00013-1.

Mao, Y., Li, X., Smyth, E.M., Yannarell, A.C., Mackie, R.I., 2014. Enrichment of specific bacterial and eukaryotic microbes in the rhizosphere of switchgrass (Panicum virgatum L.) through root exudates. Environmental Microbiology Reports 6, 293–306. https://doi.org/10.1111/1758-2229.12152.

Marchus, K.A., Blankinship, J.C., Schimel, J.P., 2018. Environmental controls on extracellular polysaccharide accumulation in a California grassland soil. Soil Biology and Biochemistry 125, 86–92. https://doi.org/10.1016/j.soilbio.2018.07.009.

Martin, J., 1946. Microorganisms and soil aggregation. Soil Science 61, 157–166.

McGowan, A.R., Nicoloso, R.S., Diop, H.E., Roozeboom, K.L., Rice, C.W., 2019. Soil organic carbon, aggregation, and microbial community structure in annual and perennial biofuel crops. Agronomy Journal 111, 128–142. https://doi.org/10.2134/agronj2018.04.0284.

McLauchlan, K.K., Hobbie, S.E., Post, W.M., 2006. Conversion from agriculture to grassland builds soil organic matter on decadal timescales. Ecological Applications 16, 143–153. https://doi.org/10.1890/04-1650.

Moffatt, H.H., 1973. Soil Survey of Caddo County, Oklahoma. United States Department of Agriculture Soil Conservation Service, Washington, D.C.

More, T.T., Yadav, J.S.S., Yan, S., Tyagi, R.D., Surampalli, R.Y., 2014. Extracellular polymeric substances of bacteria and their potential environmental applications. Journal of Environmental Management 144, 1–25. https://doi.org/10.1016/j.jenvman.2014.05.010.

Oades, J.M., 1984. Soil organic matter and structural stability: mechanisms and implications for management. Plant and Soil 76, 319–337. https://doi.org/10.1007/BF02205590.

Ontl, T.A., Cambardella, C.A., Schulte, L.A., Kolka, R.K., 2015. Factors influencing soil aggregation and particulate organic matter responses to bioenergy crops across a topographic gradient. Geoderma 1–11. https://doi.org/10.1016/j.geoderma.2015.04.016, 255–256.

O'Brien, S.L., Jastrow, J.D., 2013. Physical and chemical protection in hierarchical soil aggregates regulates soil carbon and nitrogen recovery in restored perennial grasslands. Soil Biology and Biochemistry 61, 1–13. https://doi.org/10.1016/j.soilbio.2013.01.031.

Pal, A., Paul, A.K., 2013. Optimization of cultural conditions for production of extracellular polymeric substances (EPS) by serpentine rhizobacterium cupriavidus pauculus KPS 201 [WWW document]. Journal of Polymers. https://doi.org/10.1155/2013/692374.

Parrish, D.J., Fike, J.H., 2005. The biology and agronomy of switchgrass for biofuels. Critical Reviews in Plant Sciences 24, 423–459. https://doi.org/10.1080/07352680500316433.

Pedroso, G., De Ben, C., Hutmacher, R., Orloff, S., Putnam, D., Six, J., van Kessel, C., Wright, S., Linquist, B., 2011. Switchgrass is a promising, high-yielding crop for California biofuel. California Agriculture 65, 168–173.

Petersen, D.G., Blazewicz, S.J., Firestone, M., Herman, D.J., Turetsky, M., Waldrop, M., 2012. Abundance of microbial genes associated with nitrogen cycling as indices of biogeochemical process rates across a vegetation gradient in Alaska. Environmental Microbiology 14, 993–1008. https://doi.org/10.1111/j.1462-2920.2011.02679.x.

Peterson, B.G., Carl, P., Boudt, K., Bennett, R., Ulrich, J., Zivot, E., Cornilly, D., Hung, E., Lestel, M., Balkissoon, K., Wuertz, D., 2018. Performance Analytics: Econometric Tools for Performance and Risk Analysis.

Pett-Ridge, J., Firestone, M.K., 2017. Using stable isotopes to explore root-microbe-mineral interactions in soil. Rhizosphere, New Understanding of Rhizosphere Processes Enabled by Advances in Molecular and Spatially Resolved Techniques 3, 244–253. https://doi.org/10.1016/j.rhisph.2017.04.016.

Potthoff, M., Dyckmans, J., Flessa, H., Beese, F., Joergensen, R.G., 2008. Decomposition of maize residues after manipulation of colonization and its contribution to the soil microbial biomass. Biology and Fertility of Soils 44, 891–895. https://doi.org/10.1007/s00374-007-0266-y.

R Core Team, 2018. R: A Language and Environment for Statistical Computing. R Foundation for Statistical Computing, Vienna, Austria.

Redmile-Gordon, M.A., Brookes, P.C., Evershed, R.P., Goulding, K.W.T., Hirsch, P.R., 2014. Measuring the soil-microbial interface: extraction of extracellular polymeric substances (EPS) from soil biofilms. Soil Biology and Biochemistry 72, 163–171. https://doi.org/10.1016/j.soilbio.2014.01.025.

Redmile-Gordon, M.A., Evershed, R.P., Hirsch, P.R., White, R.P., Goulding, K.W.T., 2015. Soil organic matter and the extracellular microbial matrix show contrasting responses to C and N availability. Soil Biology and Biochemistry 88, 257–267. https://doi.org/10.1016/j.soilbio.2015.05.025.

Roberson, E.B., 1991. Extracellular Polysaccharide Production by Soil Bacteria : Environmental Control and Significance in Agricultural Soil. University of California, Berkeley.

Roberson, E.B., Firestone, M.K., 1992. Relationship between desiccation and exopolysaccharide production in a soil Pseudomonas sp. Applied and Environmental Microbiology 58, 1284–1291.

Roberson, E.B., Shennan, C., Firestone, M.K., Sarig, S., 1995. Nutritional management of microbial polysaccharide production and aggregation in an agricultural soil. Soil Science Society of America Journal 59, 1587–1594. https://doi.org/10.2136/sssaj1995.03615995005900060012x.

Robertson, G.P., Hamilton, S.K., Barham, B.L., Dale, B.E., Izaurralde, R.C., Jackson, R.D., Landis, D.A., Swinton, S.M., Thelen, K.D., Tiedje, J.M., 2017. Cellulosic biofuel contributions to a sustainable energy future: choices and outcomes. Science 356, eaal2324. https://doi.org/10.1126/science.aal2324.

Rodrigues, R.R., Moon, J., Zhao, B., Williams, M.A., 2017. Microbial communities and diazotrophic activity differ in the root-zone of Alamo and Dacotah switchgrass feedstocks. GCB Bioenergy 9, 1057–1070. https://doi.org/10.1111/gcbb.12396.

Rosseel, Y., 2012. Lavaan: an R package for structural equation modeling. Journal of Statistical Software 48, 1–36.

Sandhya, V., Ali, SkZ., 2015. The production of exopolysaccharide by Pseudomonas putida GAP-P45 under various abiotic stress conditions and its role in soil aggregation. Microbiology 84, 512–519. https://doi.org/10.1134/S0026261715040153.

Schimel, J.P., 2018. Life in dry soils: effects of drought on soil microbial communities and processes. Annual Review of Ecology, Evolution, and Systematics 49, 409–432. https://doi.org/10.1146/annurev-ecolsys-110617-062614.

Sheng, G.P., Yu, H.Q., Yue, Z., 2006. Factors influencing the production of extracellular polymeric substances by Rhodopseudomonas acidophila. International Biodeterioration & Biodegradation, Surface Adhesion and Biotechnological Applications 58, 89–93. https://doi.org/10.1016/j.ibiod.2006.07.005.

Sheng, G.-P., Yu, H.-Q., Li, X.-Y., 2010. Extracellular polymeric substances (EPS) of microbial aggregates in biological wastewater treatment systems: a review. Biotechnology Advances 28, 882–894. https://doi.org/10.1016/j.biotechadv.2010.08.001.

Shipley, B., 2016. Cause and Correlation in Biology: A User's Guide Path Analysis, Structural Equations and Causal Inference with R, second ed. Cambridge University Press.

Singer, M.J., Southard, R.J., Warrington, D.N., Janitzky, P., 1992. Stability of synthetic sand-clay aggregates after wetting and drying cycles. Soil Science Society of America Journal 56, 1843–1848. https://doi.org/10.2136/sssaj1992.03615995005600060032x.

Six, J., Paustian, K., 2014. Aggregate-associated soil organic matter as an ecosystem property and a measurement tool. Soil Biology and Biochemistry 68, A4–A9. https://doi.org/10.1016/j.soilbio.2013.06.014.

Six, J., Elliott, E.T., Paustian, K., 2000. Soil macroaggregate turnover and microaggregate formation: a mechanism for C sequestration under no-tillage agriculture. Soil Biology and Biochemistry 32, 2099–2103. https://doi.org/10.1016/S0038-0717(00)00179-6.

Staudt, A.K., Wolfe, L.G., Shrout, J.D., 2012. Variations in exopolysaccharide production by Rhizobium tropici. Archives of Microbiology 194, 197–206. https://doi.org/10.1007/s00203-011-0742-5.

Thomason, W.E., Raun, W.R., Johnson, G.V., Taliaferro, C.M., Freeman, K.W., Wynn, K.J., Mullen, R.W., 2005. Switchgrass response to harvest frequency and time and rate of applied nitrogen. Journal of Plant Nutrition 27, 1199–1226. https://doi.org/10.1081/PLN-120038544.

Tiemann, L.K., Grandy, A.S., 2015. Mechanisms of soil carbon accrual and storage in bioenergy cropping systems. GCB Bioenergy 7, 161–174. https://doi.org/10.1111/gcbb.12126.

Tilman, D., Hill, J., Lehman, C., 2006. Carbon-negative biofuels from low-input high-diversity grassland biomass. Science 314, 1598–1600. https://doi.org/10.1126/science.1133306.

Tisdall, J.M., Oades, J.M., 1982. Organic matter and water-stable aggregates in soils. Journal of Soil Science 33, 141–163. https://doi.org/10.1111/j.1365-2389.1982.tb01755.x.

Upadhyay, S., S Singh, J., Singh, D.P., 2011. Exopolysaccharide-Producing plant growth-promoting rhizobacteria under salinity condition. Pedosphere 21, 214–222.

Venables, W.N., Ripley, B.D., 2002. Modern applied statistics with S. In: Statistics and Computing, fourth ed. Springer, New York.

Waldrop, M.P., Firestone, M.K., 2006. Seasonal dynamics of microbial community composition and function in oak canopy and open grassland soils. Microbial Ecology 52 (3), 470–479. https://doi.org/10.1007/s00248-006-9100-6.

Wang, J., Yu, H.-Q., 2007. Biosynthesis of polyhydroxybutyrate (PHB) and extracellular polymeric substances (EPS) by Ralstonia eutropha ATCC 17699 in batch cultures. Applied Microbiology and Biotechnology 75, 871–878. https://doi.org/10.1007/s00253-007-0870-7.

Wang, S., Redmile-Gordon, M., Mortimer, M., Cai, P., Wu, Y., Peacock, C.L., Gao, C., Huang, Q., 2019. Extraction of extracellular polymeric substances (EPS) from red soils (Ultisols). Soil Biology and Biochemistry 135, 283–285. https://doi.org/10.1016/j.soilbio.2019.05.014.

Wickham, H., 2016. ggplot2: Elegant Graphics for Data Analysis, second ed. Use R! Springer, Cham.

Wolfaardt, G.M., Lawrence, J.R., Korber, D.R., 1999. Function of EPS. In: Wingender, J., Neu, T.R., Flemming, H.-C. (Eds.), Microbial Extracellular Polymeric Substances. Springer.

Yeats, T.H., Sorek, H., Wemmer, D.E., Somerville, C.R., 2016. Cellulose deficiency is enhanced on hyper accumulation of sucrose by a H+-Coupled sucrose symporter. Plant Physiology 171, 110–124. https://doi.org/10.1104/pp.16.00302.

Zhalnina, K., Louie, K.B., Hao, Z., Mansoori, N., Rocha, U.N. da, Shi, S., Cho, H., Karaoz, U., Loqué, D., Bowen, B.P., Firestone, M.K., Northen, T.R., Brodie, E.L., 2018. Dynamic root exudate chemistry and microbial substrate preferences drive patterns in rhizosphere microbial community assembly. Nature Microbiology 3, 470. https://doi.org/10.1038/s41564-018-0129-3.

Zuur, A.F., Ieno, E.N., Elphick, C.S., 2010. A protocol for data exploration to avoid common statistical problems. Methods in Ecology and Evolution 1, 3–14. https://doi.org/10.1111/j.2041-210X.2009.00001.x.